AD NUMBER

AD826187

NEW LIMITATION CHANGE

TO

Approved for public release, distribution unlimited

FROM

Distribution authorized to U.S. Gov't. agencies and their contractors; Operational and Administrative Use; Oct 1967; Other requests shall be referred to Army Electronics Command, Fort Monmouth, NJ.

AUTHORITY

USAEC ltr, 30 Jul 1971

AD

Research and Development Technical Report

ECOM-2900

COMMUNICATION AND TARGET DETECTION THROUGH ICE BY MEANS OF SEISMIC ACOUSTIC SIGNALS

by

K. Ikrath
R. F. Johnson
W. Kennebeck
K. J. Murphy
R. Ridgeway
L. Stascavage

October 1967

ECOM

UNITED STATES ARMY ELECTRONICS COMMAND · FORT MONMOUTH, N.J.

54

NOTICES

Disclaimers

The findings in this report are not to be construed as an official Department of the Army position, unless so designated by other authorized documents.

The citation of trade names and names of manufacturers in this report is not to be construed as official Government indorsement or approval of commercial products or services referenced herein.

Disposition

Destroy this report when it is no longer needed. Do not return it to the originator.

REPORTS CONTROL SYMBOL OSD-1366

RESEARCH AND DEVELOPMENT TECHNICAL REPORT

ECOM - 2900

COMMUNICATION AND TARGET DETECTION THROUGH ICE BY MEANS OF SEISMIC ACOUSTIC SIGNALS

by

Kurt Ikrath, Ronald F. Johnson,
William Kennebeck, and Kenneth J. Murphy

Institute for Exploratory Research
U. S. Army Electronics Command
Fort Monmouth, N. J.

and

Robert Ridgeway and Leonard Stascavage

Naval Ordnance Laboratory
Silver Spring, Maryland

OCTOBER 1967
DA TASK No. 1PO 14501 B31A 01 43

U. S. ARMY ELECTRONICS COMMAND
FORT MONMOUTH, N. J.

ABSTRACT

Seismic-acoustic signal transmission experiments, employing novel seismic transducers on land and lake ice as transmitters and conventional hydrophones in water beneath the ice as receivers, are described. The observed influences of wave excitation and propagation phenomena on the signal character of transmissions through earth, ice, and water are discussed. Applications of seismic-acoustic systems for communications and target detection are indicated.

FOREWORD

Research was performed and authorized under DA 0A1743, AMC Code 5011 11 854 01 Project/Task No. 1P0 14501 B31A 01, "Research in Electronics - ECOM."

Mr. M. M. Kleinermann of the Naval Ordnance Laboratory conceived the idea of using experimental seismic systems for communication with and detection of submarines submerged beneath solid ice covers in arctic seas.

Contributions by Mr. W. Schneider relative to the design of seismic transducers and Mr. G. LeMeune relative to the mechanical construction of transducers and ancillary equipments are gratefully acknowledged. The Seismic Communication Research Team of Division C, Institute for Exploratory Research extends thanks to Mr. A. Zanella, ECOM, who assisted in setting up and operating the electrical instrumentation and Miss Anne Stommel for her assistance in the preparation of this report.

Special thanks are due Capt. Clifford Schumann, U. S. Air Force Liaison Officer, USAECOM, for his efforts in obtaining permission from the Wade Co., Keesville, New York to use its property for access to Lake Champlain for experiments with seismic transmissions.

CONTENTS

FIGURES

COMMUNICATION AND TARGET DETECTION THROUGH ICE BY MEANS OF SEISMIC ACOUSTIC SIGNALS

INTRODUCTION

A high level of perfection has been attained in sonar and accustic underwater communication systems in open seas. In ice-covered arctic waters, however, interference caused by acoustic noise emanating from moving and bursting ice affects the performance of these systems. The operational requirement that acoustic devices must first be inserted through ice, and then immersed into water, also makes existing systems far from perfect.

In submarine rescue operations in the Arctic, holes must be drilled through the ice before immersing hydrophone detectors or the applicable sources necessary for detection of and/or communication with submarines submerged below the ice cover. Time spent drilling these holes could be better used in finding the vessel and saving lives. Hence, an urgent need exists for efficient seismic-acoustic devices and techniques by which signals can be transmitted via ice into water, and received via water on the ice.

Further, it is necessary to communicate by seismic-acoustic means from underground command installations to the surface. Low-frequency seismic signals are able to penetrate the upper weathered layers of the earth and soil overburden; however, in the case of underground hardened sites such as mines or tunnels, the stress-stiffened walls inhibit radiation and upward transmission. In the case of high-frequency transmissions, the extremely absorbent weathered layer blocks transmissions from reaching the surface; however, high-frequency signals do penetrate sediment layers on the bottoms of lakes and can be received in water by hydrophones. It is necessary to transmit and receive seismic-acoustic signals via both land and water to implement a "Hard-Line" communications system. Such a seismic-acoustic system will permit communication between surface or underground installations on the coast and submarines submerged offshore.

The seismic-acoustic experiments described in this report are the first phase in the development of a seismic-acoustic system for communication and detection between the earth and ice-covered water.

DISCUSSION

Development of the Concept

The idea of using an experimental seismic communications system for application to submarine communications in the Arctic was conceived by M. M. Kleinermann of the Naval Ordnance Laboratory, Silver Spring, Maryland.[1] Implementation of this idea was accomplished by modification of equipments and procedures used in previous experiments during which nominal 80 Hz seismic signals were transmitted through lake ice by the flexural-wave mode.[2] The modification permitted signal reception in water, and used hydrophones immersed below the ice at various distances from the seismic transducers (XTDs) located on the surface of the ice.

In view of the difficulties usually encountered in experimental work in the Arctic, it was decided to conduct low-cost feasibility experiments on Lake Champlain in New York State (Fig. 1).

Experimental Setup and Instrumentation

A van housing seismic communications instruments was set up on the Wade Company property (Fig. 1). Two resonant seismic transducers (80 Hz, 200W) were situated 100 meters from, and 40 meters above, the surface of the lake on a flat spot at the crest of a hill (Fig. 2). Four seismic transducers (80 Hz resonant, 10 W) and an improvised version of the experimental stack transducer (Fig. 3) were placed on the ice approximately 200 meters offshore.

In communications experiments, the small (10 W) seismic transducers were deployed at 15-meter spacings in the form of a linear array oriented perpendicular to the shore. During experiments relating to obstacle scatter and detection, the small transducers were deployed in the form of a square array. Two hydrophone receivers were suspended from wooden cradles to a depth of six meters in the water below the ice. One hydrophone (Fig. 4) was centered beneath small transducers XTD-1 and XTD-2 of the array; the other was located 500 meters offshore in the direction of the array. The first hydrophone, the monitor hydrophone, will be referred to as "HP-1"; and the second, the distant hydrophone, will be referred to as "HP-2".

Throughout the experiments, transducers and hydrophones were connected by cables to the instrument van located onshore. All circuits and equipment configurations were checked while electrically energized, for possible electromagnetic stray-coupling between the transmitter and receiver cables, by lifting the transducers off the ice and the hydrophones out of the water. Zero signal levels verified proper functioning of the system.

During the course of the experiments, weather and temperature changed rapidly. Temperatures ranged from about -20°F to +20°F. High noise levels, due to the cracking of ice caused by wind gusts and temperature variations, were observed. Large pressure ridges and cracks crisscrossed the ice. Safe ice extended one mile from shore. The ice cover, 20 to 25 cm thick and very dense and hard, was transparent.

Experiments

Experiments performed during Lake Champlain tests included:

1. Transmissions of nominal 80 Hz land-to-water seismic signals from a small hill; and their reception by two hydrophones submerged to a depth of approximately six meters below the ice, and located offshore at a distance of 200 and 500 meters respectively.

2. Ice-to-water transmissions of nominal 88 Hz, 250 Hz, 1000 Hz, and band-limited voice signals from the surface of the ice at about 160 to 200 meters offshore.

3. Detection of phase variations in the 250 Hz transmissions from the ice, caused by scatter from a rubber mat lowered into the water:

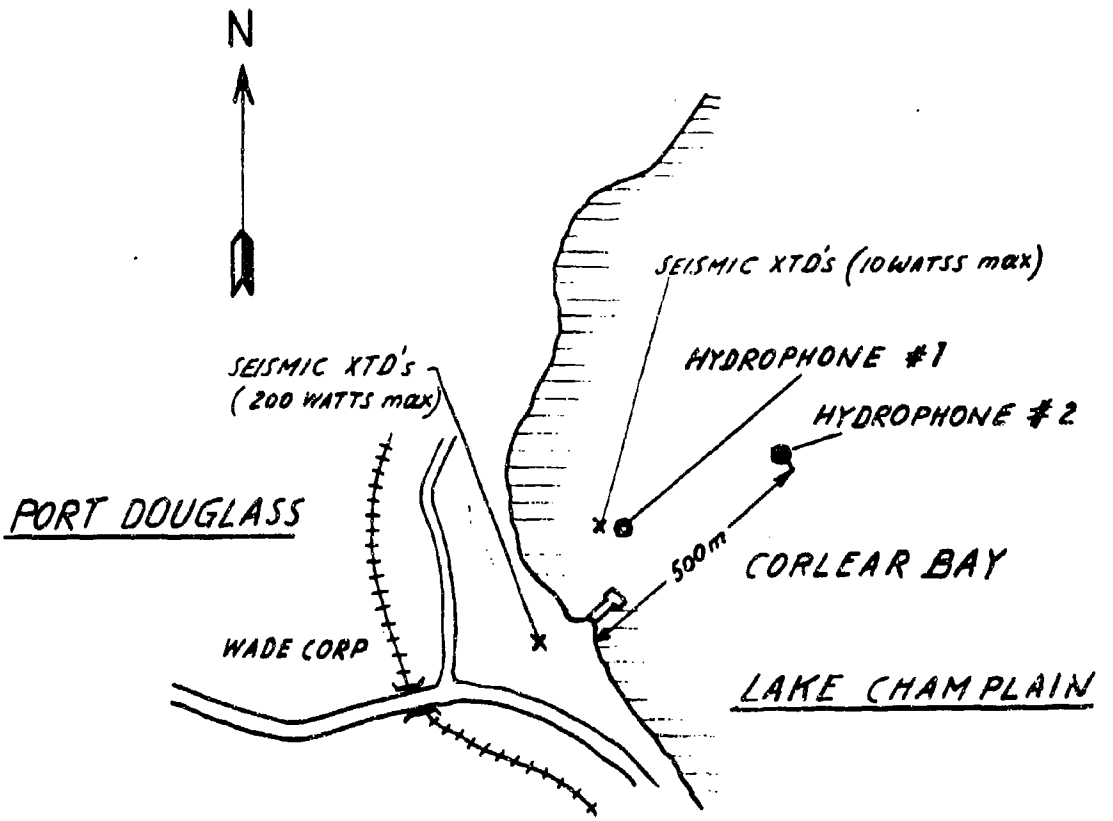

FIG. 1 MAP OF EXPERIMENT SITE AT LAKE CHAMPLAIN, NEW YORK

FIG. 2 TRANSDUCER XTD-H-1 ONSHORE

FIG. 3 STACK TRANSDUCER ON ICE

FIG. 4 CRADLE FOR HYDROPHONE HP-1

a. Beneath the transmitter site on the ice (side scatter experiments), and

b. Between transmitter and hydrophone sites respectively (forward scatter experiments).

4. Measurements of:

a. Vibration amplitudes of the ice caused by seismic transducers, and

b. The resulting acoustic pressure on hydrophones below the ice.

5. Measurement of temperature- and wind-induced acoustic noise levels within several frequency bands.

6. Determination of the effects of CO_2 gas bubbles, in water and between water and ice, on the coupling of acoustic signals transmitted from ice into water.

Organization of Data and Method of Evaluation

In view of the immediate influence of these experimental results on submarine operations in arctic ice-covered waters, all pertinent experimental data, observations, and remarks are included in the Appendices. Data from similar or repeated experiments are grouped together under one heading; therefore, log items are not in chronological order. However, time and environmental conditions for each experiment are given as "Remarks" in connection with the data. The data in Appendices A through D and the calculations in Appendices E and F form the basis for the analysis and evaluation of experimental results in regard to:

1. Submarine communications and detection in arctic ice-covered waters, and

2. Communications from hardened sites.

The method of analysis and evaluation is described by the Flow Chart given in Fig. 5.

Evaluation and Interpretation of CW and Pulsed Communications Experiments

A comparison of the experimental data presented in Appendices A and B regarding the signal quality of transmissions from land and from ice reveals that the 88 Hz transmissions from ice into water displayed the most inferior quality of any signals received during the experiments. Nominal 80 Hz transmissions from land via soil, rock, and water over a total distance of 600 meters reveals a much better signal quality than similar low-frequency (88 Hz) transmissions from the ice surface over a distance of only 300 meters. In interpreting these differences in low-frequency transmissions (80 and 88 Hz) from land and ice, it should be noted that high-frequency transmissions (250 to 1000 Hz) from the same site on the ice were far superior to the 88 Hz transmissions. Visible evidence can be seen in Figs. 6 to 11.

For example, compare Figs. 6 and 7 (the recordings of the heterodyned CW and pulse signal outputs from the distant hydrophone obtained from transmission of the 80 Hz signal from land) with Fig. 8 (the recording of the

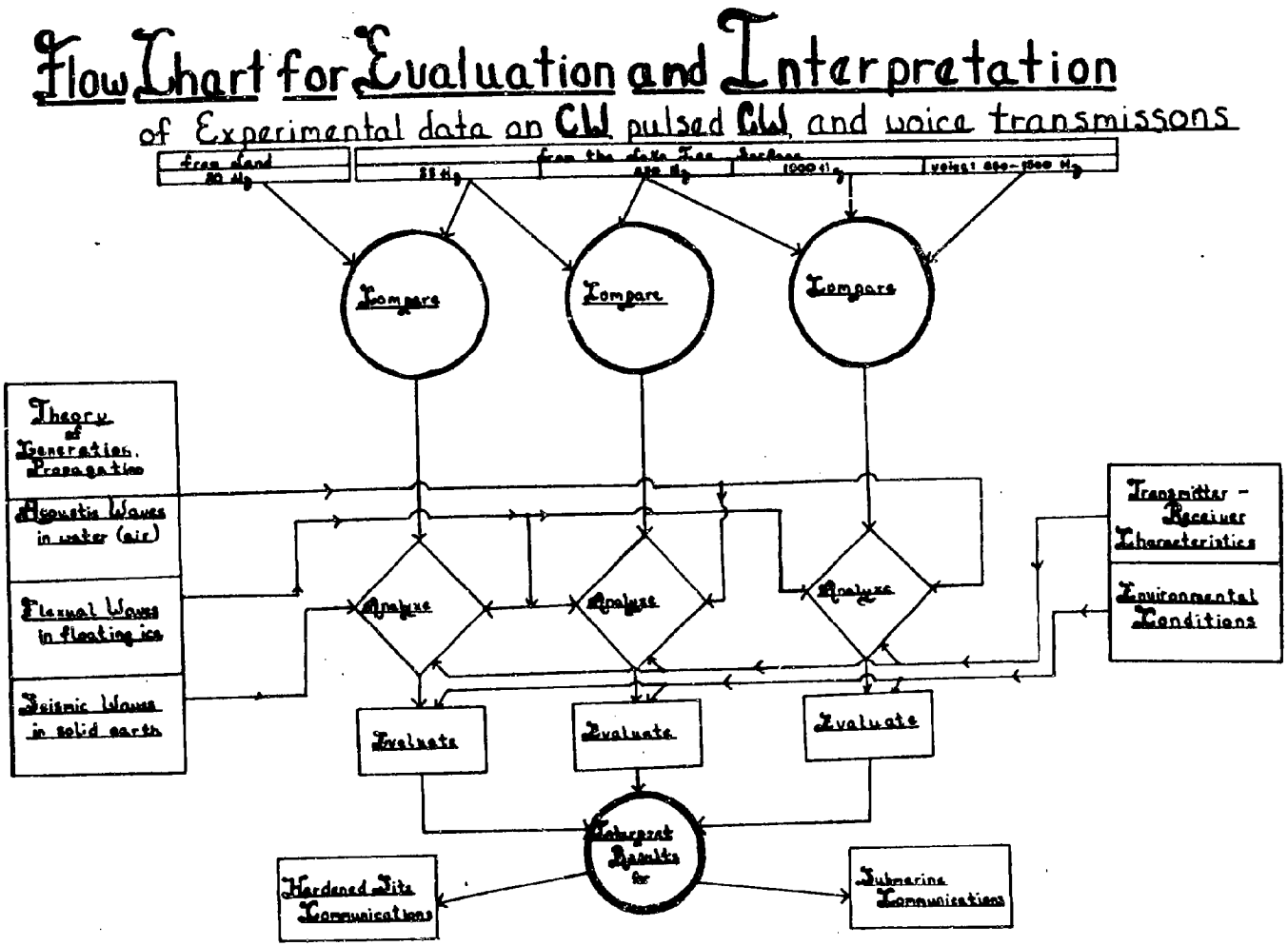

FIG. 5 LOGIC FLOW CHART FOR EVALUATION AND INTERPRETATION OF EXPERIMENTAL DATA

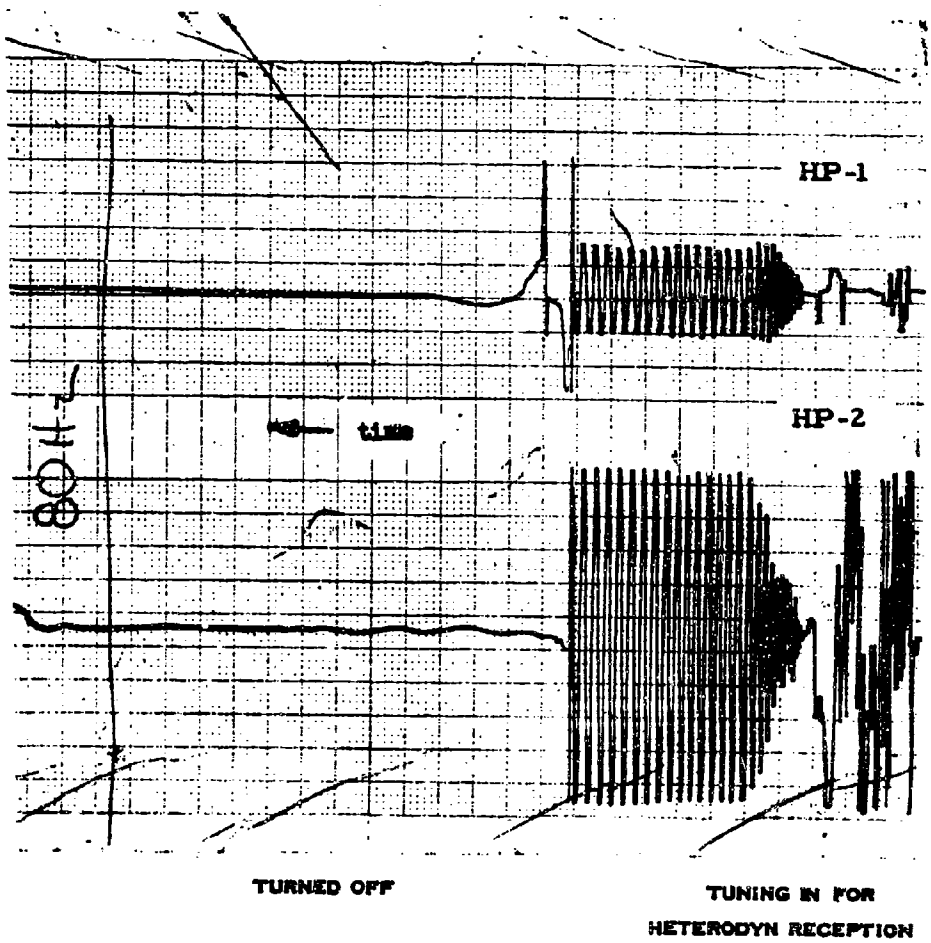

FIG. 6

SANBORN RECORDING OF 80 Hz CW TRANSMISSION FROM SHORE:
RECEPTION BY HYDROPHONES HP-1 AND HP-2

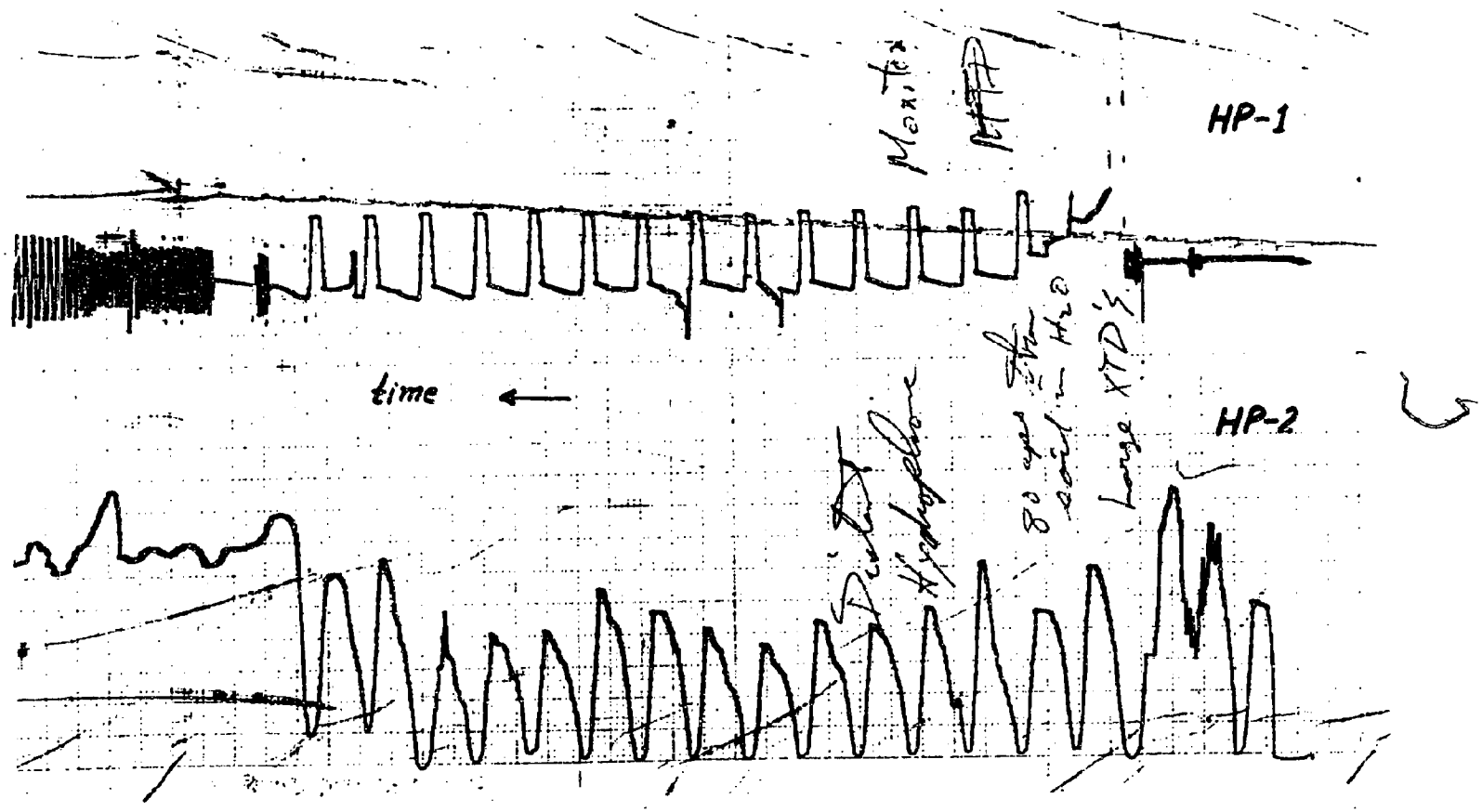

FIG. 7 SANBORN RECORDING OF PULSED 80 Hz TRANSMISSION
FROM SHORE (XTD-H-2, ALONE); RECEPTION BY HYDROPHONES HP-1 AND HP-2

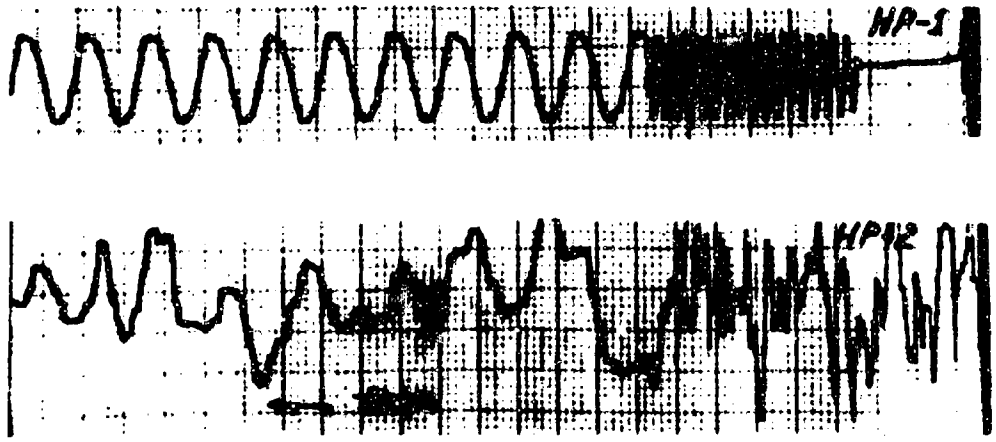

Chart speed 5 mm /sec

FIG. 8 SANBORN RECORDING OF 88 Hz CW TRANSMISSION FROM FOUR-TRANSDUCER ARRAY ON THE ICE; RECEPTION BY HYDROPHONES HP-1 AND HP-2

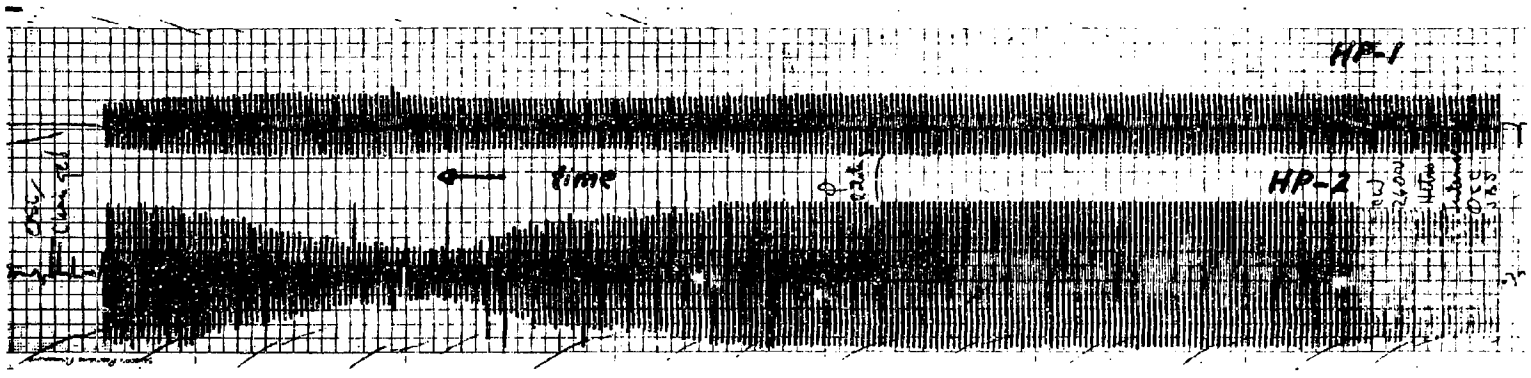

FIG. 9

SANBORN RECORDING OF 250 Hz CW TRANSMISSION FROM FOUR-TRANSDUCER ARRAY ON THE ICE (PATTERN ROTATING); RECEPTION BY HYDROPHONES HP-1 AND HP-2

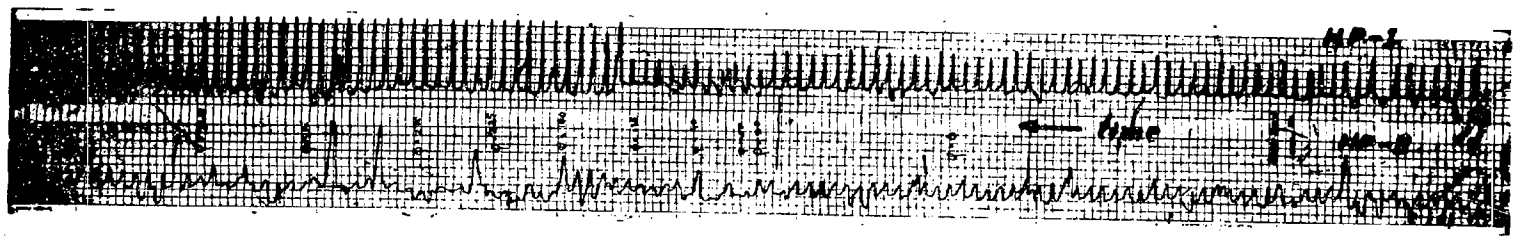

FIG. 10 SANBORN RECORDING OF PULSED 250 Hz TRANSMISSION FROM FOUR-TRANSDUCER ARRAY ON THE ICE (PATTERN PHASING INDICATED); RECEPTION BY HYDROPHONES HP-1 AND HP-2

FIG. 11 OPTICAL RECORDING OF PULSED 1000 Hz TRANSMISSION FROM STACK TRANSDUCER ON THE ICE; RECEPTION BY HYDROPHONE HP-2

88 Hz signal from the ice surface). Due to the marginal quality of the 88 Hz CW transmission from the ice-surface array of small seismic transducers, no attempt was made to record pulse-amplitude modulated signals at the same carrier frequency. In contrast, notice the recordings given in Fig. 9, which show 250 Hz CW signals transmitted from the ice surface by the same array using small seismic transducers operating in the third harmonic resonance mode. This recording (Fig. 9) clearly shows the variation in the received 250 Hz signal level as a function of phase variations in the electrical drive voltages of the array. In this case, phase variations are produced by a motor-driven phase shifter in the drive circuit of the transducer array.

Of particular interest is the fact that ice-cracking noise interference with 250 Hz transmissions is negligible when compared to the case of 88 Hz transmissions, even though ambient noise levels measured by the hydrophone in the 60 to 100 Hz frequency band are almost equal to those in the 230 and 280 Hz frequency band (Appx. B). Similar to the CW case, control over the array radiation pattern, and thus levels of the pulsed 250 Hz signals by adjustment of the phase of the array, is indicated in Fig. 10.

A direct optical recording, made by CEC Model 5-124 of the almost ideal $\frac{\sin x}{x}$ type shape of the pulsed 1000 Hz signal transmitted from the stack transducer, is seen in Fig. 11. Interference again is negligible. Evidently, high-frequency transmissions from ice are extremely well received by hydrophones in water, and are almost free of interference from ice-cracking noises. In view of the excellent reception of these essentially single-frequency signals in the voice-frequency spectrum, one would expect voice signals to be received equally well. This was not the case. Band-limited voice signals (250 to 1500 Hz) transmitted from the stack transducer came through perfectly over the monitor hydrophone beneath the transmitter site. However, voice signals picked up by the distant hydrophone were completely unintelligible. These experimental data raise the following questions:

1. Why is the 88 Hz transmission from ice inferior to the 80 Hz transmission from the more distant land? (Propagation losses are much greater in earth than in hard ice and water and, therefore, should more than offset differences in the primary power levels. Hydrophone receiver circuits were identical and ambient noise levels at hydrophone locations were almost equal in both cases).

2. Why are transmissions from the ice, of 2[illegible]z signals, superior to transmissions of 88 Hz signals? (In both cases, transmitter and receiver circuits were identical except for the filter bandwidths of receiver circuits--230 to 280 Hz and 60 to 100 Hz respectively.)

3. Why is the voice signal lost over the longer distance? (Individual frequencies in the voice spectrum -- e.g., 250 Hz and 1000 Hz -- came through well above ambient noise levels.)

Analysis shows the phenomena that are primarily involved:

1. In the case of 80 Hz signal transmission from land, via soil and rock into water:

a. Radiation of split beams of shear waves from the transducers on the hill into earth, and

b. Refraction of one of these shear-wave beams at the sloping soil-water boundary and its conversion into a pressure wave in the water.

2. In the case of transmissions from ice into water:

a. At low frequencies (88 Hz): Excitation and propagation of flexural waves in the ice, and

b. At high frequencies (250 Hz, 1000 Hz): Acoustic coupling to the water and cutoff-type attenuation of the flexural wave mode.

3. In the case of interference by ice-cracking noises:

a. At low frequencies (88 Hz): From distant cracks, predominantly via the flexural-wave mode of the ice, and

b. At high frequencies (250 Hz, 1000 Hz): Predominantly via the acoustic mode travelling through water.

Analysis of Low-Frequency Transmission Mechanisms: 80 Hz from Land vs. 88 Hz from Ice

Apparently transmission of the 80 Hz signals from land via soil, rock, and water involved an efficient mode transformation at the earth-water boundary as deduced from the following data:

1. As little as thirty watts drive power at 82 Hz, fed into land-based transducer XTD-H-2 only, yielded an output at hydrophone HP-1 of 10 millivolts corresponding to $\sim$ 1 microbar acoustic power, 11 dB above noise level (Appx. A).

2. A total of 1.8 watts drive power at 88 Hz for small ice-based transducers XTD-1 and XTD-2 in the vicinity of hydrophone HP-1 yielded an output of 86 millivolts, corresponding to $\sim$8 microbars of acoustic pressure, and an ice vibration velocity of 0.027 mm/sec at the hole for the hydrophone (Appx.B).

3. Estimate of the power balance of transmitted versus received signals:

a. It is obvious that only a small fraction of the original 30 watts fed into land-based transducer XTD-H-2 reached the hydrophone: First of all, the radiation efficiency of the transducer is at most only 25%; and secondly, the radiated power is distributed over several modes, i.e., surface-wave (Rayleigh wave) mode, subsurface pressure mode, and the shear-wave mode.[3]

b. Power going into the subsurface shear-wave mode is roughly 20% of the total radiated power. This shear-wave mode seems to play the most important role in our case. Shear waves are radiated in the form of split beams into earth in such a way that one of the beams strikes the sloping earth-water boundary at oblique angles. At such oblique angles, ranging from about 10° to 40° relative to the earth-water boundary surface, approximately 20% of the incident power is transmitted into the water. At the earth-water boundary, incident shear waves are refracted and transformed into acoustic-pressure waves travelling in a predominantly horizontal direction.

c. A comparison of land-to-water with ice-to-water transmissions of nominal 80 Hz signals, raises the question: Why does the much lower acoustic pressure (1 microbar at HP-1) in the land-to-water transmission produce signals

of a much higher quality at longer distances (HP-2) than the much higher acoustic pressure (8 microbars at HP-1) in the ice-to-water transmission?

d. The most likely reasons for the inferior quality of signals transmitted from ice over the shorter distance (300 m) are the following:

(1) A significant amount of the power is radiated by the flexural-wave mode. Flexural vibrations in ice are accompanied by acoustic waves in the water and air; however, the acoustic portion of the flexural-wave signal is ducted along the underside of the ice in such a manner that its intensity decays exponentially with depth. The signal amplitude at a depth equal to approximately the wavelength of sound in air divided by 2π is reduced to 36%. This would be, in our case, roughly 0.6 meters. Hence, the signal energy in this flexural-wave mode hardly reaches the distant hydrophones at a depth of about 6 meters.

(2) One may conclude, therefore, that the hydrophones are strongly decoupled from ice-cracking noise propagated by the flexural-wave mode. This is correct for the hydrophones, but not for the transducers based on the ice. We have, then, the curious situation in which ice noise enters into transmissions at the transmitter. It happens that ice noise is very strong in transmissions at $\sim$88 Hz. It is at these frequencies that the audible ice-cracking bursts are propagated over long distances by air-coupled flexural waves.[4]

(3) Thus, ice-based transducers are energized mechanically by flexural noise vibrations of the ice, and electrically by the signal source. This, then, explains the inferior quality of low-frequency signals transmitted from ice as compared with those transmitted from land.

Analysis of the Transmission Mechanisms: High-Frequency vs. Low-Frequency Transmissions from Ice into Water

The superior quality of high-frequency transmissions (250 Hz, 1000 Hz) relative to the low-frequency transmission (88 Hz) is intimately connected with the attenuation of flexural waves as a function of frequency. Above a critical frequency, the attenuation of flexural-wave modes in ice approaches a cutoff condition. This critical frequency is approximately 10% above the frequency at which the spectrum of the air-coupled wave reaches a sharp peak (flexural-wave propagation velocity in the ice then equals sound propagation velocity in the air). The approximate value of this critical frequency in Hz is given by:[4]

$$f_c \cong \frac{0.3}{\text{Ice Thickness in Meters}} \cdot 10^2 .$$

In our case, for ice that is 20 and 25 cm thick, $f_c \leq 150$ Hz. Thus, at higher signal frequencies (250 Hz, 1000 Hz), distant noise, caused by ice cracking and propagated by the flexural-wave mode, is almost suppressed. Signals are radiated effectively through water via the acoustic-wave mode only, and any superimposed low-frequency noise from flexural vibrations of the ice at the transmitter site is removed by filtering. Hence, the superior quality of high-frequency over low-frequency signals.

Signal Frequency Bandwidths and Noise Bandwidths

Filter bandwidths used for reception of low-frequency signals were from 60 to 100 Hz, and from 60 to 120 Hz (Appendices A and B). Therefore, filter

bandpasses were located in the spectrum where the most severe flexural noise vibrations of the ice surface occur. For reception of 250 Hz and 1000 Hz transmissions, filter bandpasses were used of 230 and 280 Hz, and 900 to 1100 Hz, respectively. Considering that the bandwidth of pulsed (on-off) CW signals is less than 10 Hz, further improvements in the signal-to-noise ratios of received signals are certainly possible by reduction of these filter bandwidths.

The following fact is important. Ambient noise levels within these frequency bands, as measured by the hydrophones, were of the same order of magnitude (Appx. B). However, as pointed out previously, received signal-to-noise ratios of the high-frequency transmissions were much superior to those of the low-frequency transmissions. This is further confirmation that interference from ice noise enters into low-frequency transmissions at the transmitter site on the ice.

Evaluation and Interpretation of Results of Voice Communications Experiments

An attempt to receive voice signals in the 250 to 1500 Hz band failed, in spite of the fact that the voice coming over the monitor hydrophone was loud and clear. Apparently over long distances, voice signals are not only degraded by noise but also garbled by the dispersive propagation of voice frequencies. This conclusion is derived from the fact that single 250 and 1000 Hz CW and pulsed CW signals were received by the distant hydrophones at signal-to-noise ratios of approximately 30 dB (Appx. B). This dispersion of voice signals is caused by frequency- and angle-dependent reflections and refractions of acoustic waves at the ice and the sedimentary bottom of the lake.[5]

Evaluation and Interpretation of Results of Side-Scatter and Forward-Scatter Experiments: Detection of Floating Objects beneath the Ice

The method of detecting floating objects beneath ice by scatter-induced variations of the phase of the CW signal transmission is an extension of the "Seismic Fence" Intrusion Detection System.[6] Instead of a seismic transducer, a hydrophone was used for reception of the signal emitted from the small seismic transducers located on the ice. The intrusion of an object floating beneath the ice into the acoustic beam emanating from the ice-based transducers was detected by the resultant change in phase of the received signal relative to the transmitted signal.

A foam-rubber mat about 1 meter wide, 2 meters long, and 1.5 cm thick was used as the scatter object. This compliant rubber mat was fastened to a rope, pushed through a small hole in the ice, and lowered into the water. Two old batteries were attached to the mat and served as ballast to offset buoyancy. The choice of a thin sheet of foam rubber as a scatter object was dictated by requirements of: First, compliancy, i.e., being able to force a large object through small holes; and secondly, sound absorbency.

Side Scatter vs. Forward Scatter

1. Side-Scatter Experiments (Fig. 12)

a. Scatter-induced phase variations of the 250 Hz CW transmissions as a function of depth of the foam-rubber mat are recorded in Fig. 13. Peak

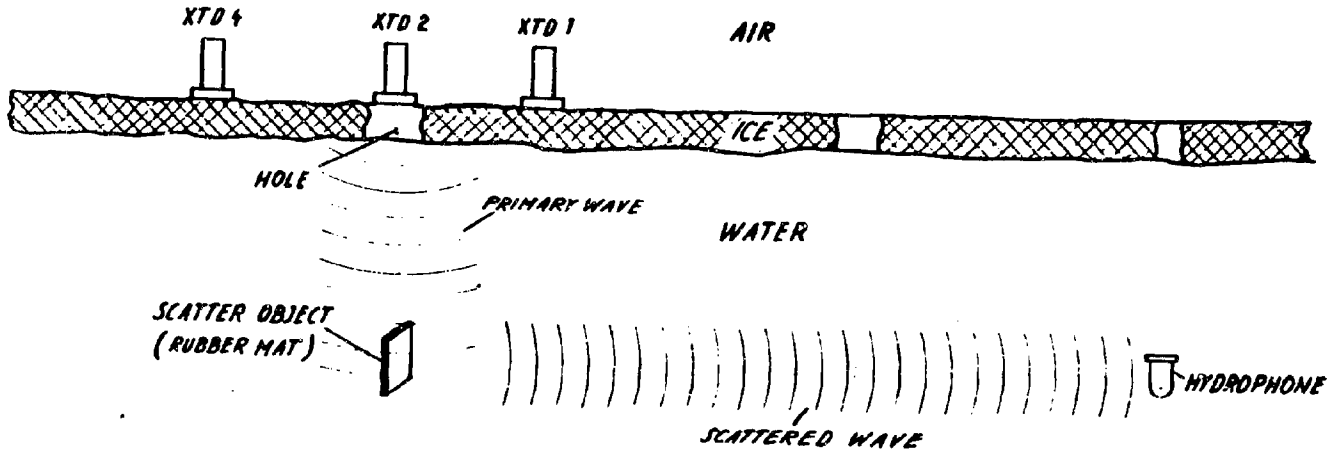

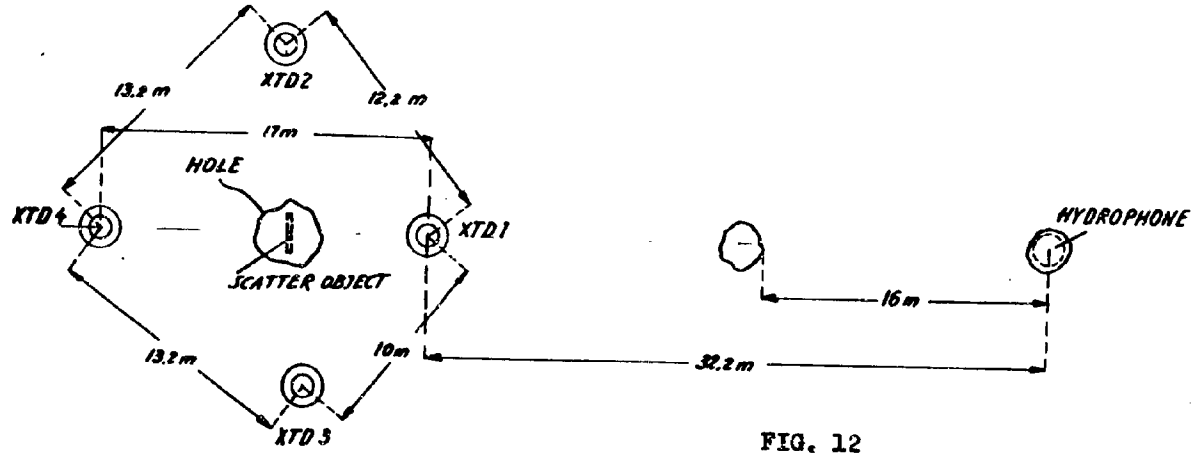

FIG. 12
DIAGRAM OF SIDE-SCATTER EXPERIMENT

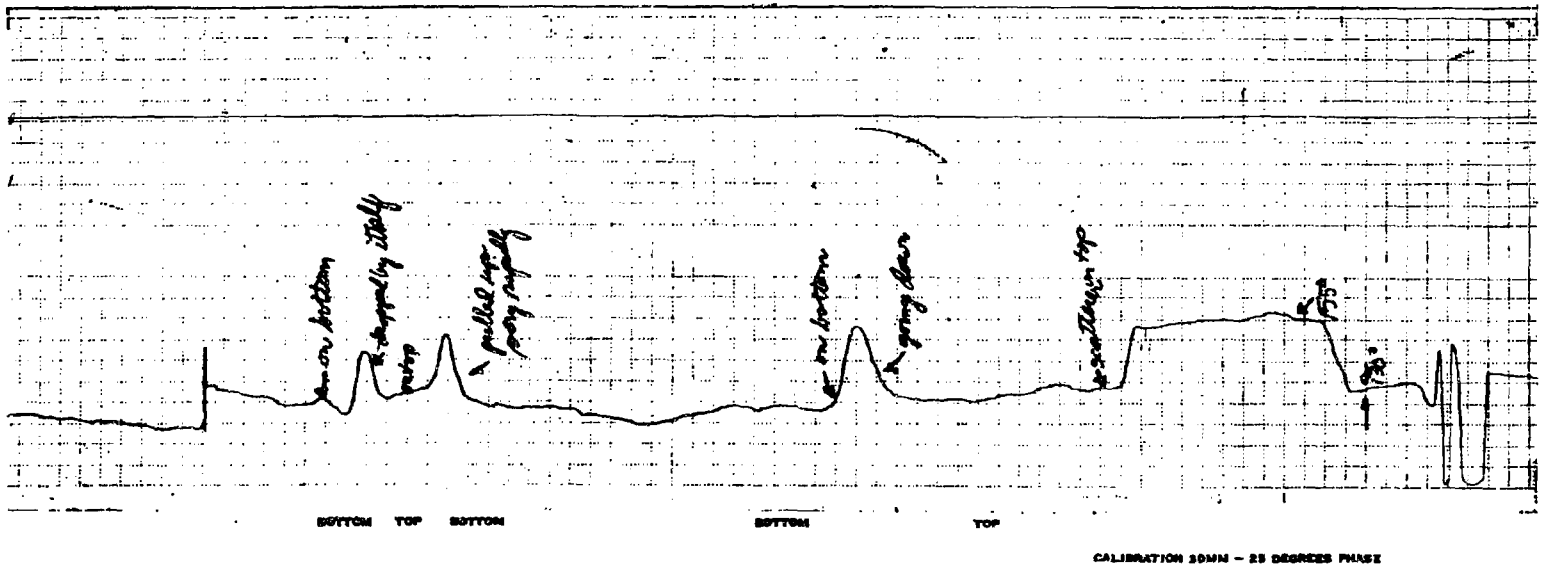

FIG. 13 SANBORN RECORDING OF 250 Hz CW PHASE VARIATIONS
vs DEPTH OF RUBBER MAT OBSTACLE IN SIDE-SCATTER EXPERIMENT

deviations from the original phase balance between transmitted and received signals are 25 degrees. (See calibration at the beginning of the experiment as shown on the right-hand side of the recording in Fig. 13, 30 mm = 25°.) Maximum phase levels occurred when the foam-rubber mat was halfway between the ice cover and the sedimentary bottom of the lake. The phase curve is single-humped. Phase levels corresponding to a bottom or top location of the foam-rubber mat in the water are almost equal -- the difference being 2.5 degrees. The phase curve is perfectly reproducible (Fig. 13).

b. For analysis, it is necessary to emphasize that in this side-scatter case, the foam-rubber mat was moved up and down beneath the transmitter site within a maximum of the radiation pattern of the square array of seisic transducers on the ice surface. The distant hydrophone receiver, on the other hand, was within a minimum of this acoustic radiation pattern which was achieved by adjusting the phase relations between the electrical drive voltages of the transducers with a four-channel phase shifter.

2. Forward-Scatter Experiments

The experimental setup was different in the forward-scatter case. Only one seismic transducer was used as a transmitter. The foam-rubber mat was moved up and down in the water at a location about halfway between the transmitter on the ice and the hydrophone receiver. The resultant phase variations, as a function of the depth of the mat, were now double-humped (Fig.14). Phase variations went through zero when the foam-rubber mat was approximately in line with the transducer on the ice and hydrophone. Now, phase levels obtained with the mat situated below the ice were distinctly different from those obtained when the mat was lying on the bottom of the lake.

3. Analysis of the Results of Scatter Experiments

a. A detailed analytical explanation for recorded phase variations of the CW signal as a function of the position of the foam-rubber mat is given in Appendix E. This theoretical analysis confirms the fact that the foam-rubber mat represented an absorber-type scatter body. The scatter radiation pattern of such a body has a minimum (null) in the direction of the incident wave, hence, the double-humped shape of the phase variation as a function of the depth of the rubber mat in the forward-scatter experiment.

b. On the other hand, a maximum was obtained in a direction perpendicular to the incident wave, hence, the single-humped shape of the phase variation as a function of depth of the rubber mat in the side-scatter experiment.

c. Levels of phase curves associated with a top or bottom location of the rubber mat are related to variable responses of the sedimentary bottom to vertically incident, or obliquely incident, acoustic waves.

d. When the rubber mat is lying on the sedimentary bottom beneath the transmitter site (side-scatter experiment), both the rubber mat and the sedimentary bottom absorb the vertical incident waves. However, oblique incident waves (side-scatter experiment) are reflected by the sedimentary bottom, and absorbed by the rubber mat. At the underside of the ice, the acoustic contrast between the reflecting ice and the absorbent rubber mat is largely a

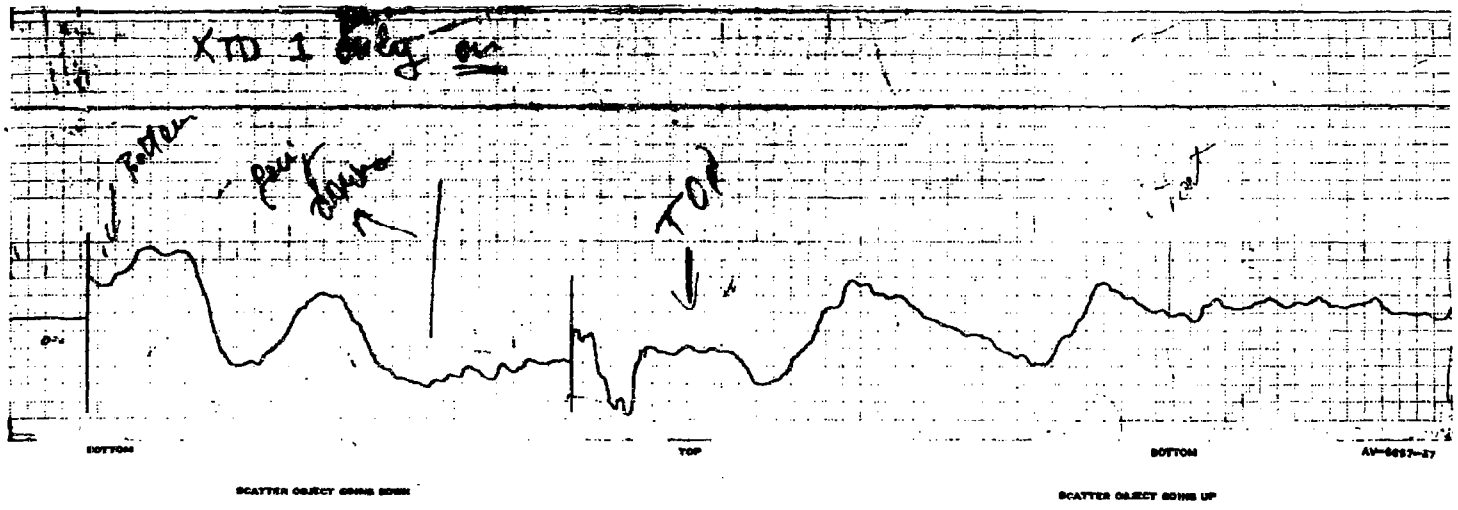

FIG. 14

SANBORN RECORDING OF 250 Hz CW PHASE VARIATIONS vs DEPTH OF RUBBER MAT OBSTACLE IN FORWARD-SCATTER EXPERIMENT

function of orientation of the rubber mat relative to the direction of the incident acoustic wave (parallel in the side-scatter case, and perpendicular in the forward-scatter case).

Effects of Air Bubbles and Sheets of Air between Ice and Water

Carbon dioxide emitted from a fire extinguisher was used to simulate conditions wherein a large sheet of air is trapped below the ice at the transmitter site. The formation of a sheet of CO_2 gas almost three meters in diameter had no significant effect on levels of the 250 Hz CW signals emitted from the small transducers. Bubble-induced phase changes are recorded in Fig. 15. Noise disturbances were observed while the CO_2 gas was being blown into the water; however, once the bubbles settled at the underside of the ice, no further interference occurred.

CONCLUSIONS

1. The seismic transducers and techniques developed for communication through earth media are applicable for communications from the surface of floating ice to submerged submarines. Transmission frequencies must be higher than the critical frequency associated with the response of flexural vibrations to noise due to the cracking and bursting of the ice. Using only 2 to 3 watts of power, narrow-band signals with carrier frequencies of 250 Hz (third harmonic of the fundmental frequency of the small seismic transducers) and 1000 Hz (stack transducer) were transmitted from ice into water and received by submerged hydrophones. Transmission and reception of voice signals in the 250 Hz to 1500 Hz band over a long distance failed. Intelligible voice reception was possible only by the hydrophone submerged beneath the transmitter site.

2. The seismic transducers and techniques employed are applicable to seismic-acoustic communications from land, via earth and water, to submerged submarines.

a. Narrow-band nominal 80 Hz signals were transmitted from a hill to hydrophones submerged beneath ice in the lake, 200 meters and 500 meters offshore, respectively. A minimum of 30 watts yielded an 11 dB signal-to-noise ratio at the location 200 meters offshore and 6 meters beneath the lake ice cover. Further improvements should be readily obtainable by reduction of the bandwidth of the hydrophone circuits from 40 Hz to 5 Hz.

b. In open water, where no noise due to ice cracking occurs, acoustic interference levels are much lower and, consequently, signal power requirements are correspondingly less.

3. The "Seismic Fence" Intrusion Detection System[6] is capable of detecting objects floating in water beneath a solid ice cover. A foam-rubber mat was pushed through a hole in the ice into the water. This rubber mat induced a scatter of the 250 Hz CW signals radiated from seismic transducers on the ice, and resulted in variations of the phase of the received, relative to the transmitted, signals. These scatter-induced phase variations of up to 25° were measured as a function of the depth and location of the rubber mat beneath the ice. Theoretical values corresponding to these scatter-induced phase variations have been calculated and are given in Appendix E.

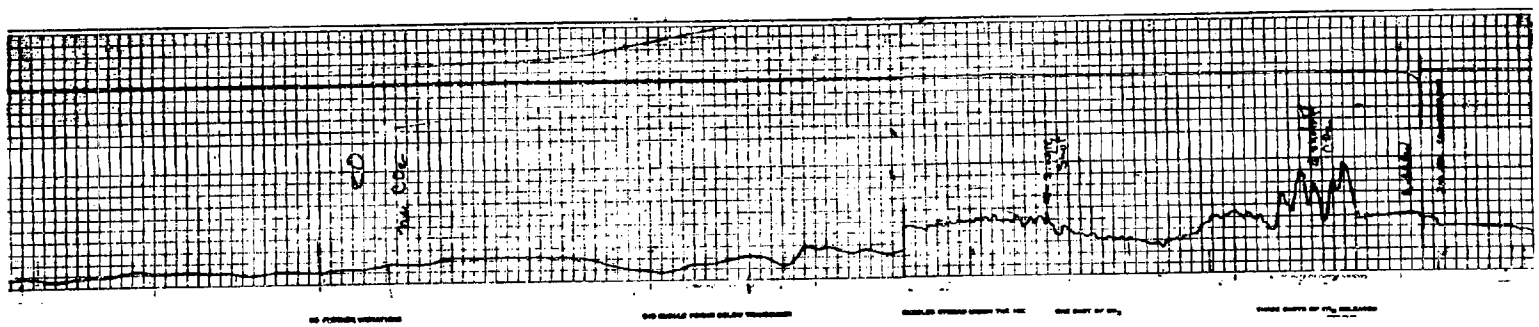

FIG. 15

SANBORN RECORDING OF 250 Hz CW PHASE VARIATIONS INDUCED BY TRAPPED GAS BUBBLES

REFERENCES

1. K. Ikrath and W. Schneider, "The Realization of Active Seismic Systems and Their Practical Applications," USAELRDL Technical Report 2446, April 1964 (AD Number 601427).

2. W. Kennebeck, "Excitation of Flexural Waves in Lake Ice With 80-Hz Resonant Seismic Transducers," Technical Report ECOM-2735, July 1966 (AD Number 639945).

3. K. Ikrath, W. A. Schneider, and R. F. Johnson, "Active Seismic Systems for Communications and Surveillance," Technical Report ECOM-2695, April 1966 (AD Number 632082).

4. W. M. Ewing, W. S. Jardetzky, and F. Press, "Elastic Waves in Layered Media," McGraw-Hill Series in the Geological Sciences, McGraw-Hill Book Company, Inc., New York, 1957.

5. J. E. White, "Seismic Waves: Radiation, Transmission, and Attenuation," McGraw-Hill, Inc., New York, 1965.

6. K. J. Murphy and K. Ikrath, "Analysis of a "Seismic Fence" For Intrusion Detection," Technical Report ECOM-2848, May 1967 (AD Number 658654).

APPENDIX A (DATA FROM LOG BOOK)

SIGNALS TRANSMITTED FROM ONSHORE VIA SOIL AND ROCK INTO WATER

DESCRIPTION OF SITES

1. Transmitter Site: A flat area on the slope of a hill about 100 meters from the beach, and 40 meters above the lake (Fig. 2).

2. Site Preparation: None. Transducers placed directly on snow-covered, frozen soil, the worst possible coupling condition. The abbreviations XTD-H-1 and XTD-H-2 refer to high power transducers.

3. Receiver Sites: Hydrophone detector HP-1, the monitor hydrophone, 200 m offshore; and HP-2, the distant hydrophone, 500 m offshore; both located at a depth of 6 to 8 meters beneath the 20 to 25 cm thick ice of the lake (Fig. 4). Water depth at hydrophone sites 30 m and 50 m respectively. The hydrophone signal (Hs) measuring and recording equipment was located onshore in the van and connected via cables.

EXPERIMENTAL DATA: SIGNAL CHARACTERISTICS, EQUIPMENT CONFIGURATIONS

Category 1:

Transmission: 80 Hz CW; rotating pattern (variable phasing of XTD-H-1 relative to XTD-H-2 drive voltage).

Transmitter: Two-transducer array.

Drive Power: 35 watts each.

Detection: By HP-1, 200 m offshore.

Received Signal: Hs = 8 mV (approximately 0.8 microbars). Received signal level written in the log book without marking corresponding phasing of XTD-1 and XTD-2. This was not the maximum received signal.

Ambient Noise: Hs = 2 mV.

SKL Filter Setting: 60 to 100 Hz, Keithly amplifier (0 dB) ahead of Ballantine meter.

Observation: Pattern rotation perfect; Phase shift: clean and clear.

Evaluation: $\frac{S+N}{N} = 20 \log \frac{8}{2} = 12$ dB.

Remarks: Date: 21 February 1967; Temperature: 0 to 10°F. Very short feasibility test.

Category 2:

Transmission: 80 Hz CW, Rotating pattern.

Transmitter: Two-transducer array.

Drive Power: Approximately 60 watts and 70 watts respectively.

Detection: By HP-1 and HP-2.

SKL Filter Setting: 60 to 120 Hz; Keithly amplifier (+20 dB) for the recording of signals by an optical recorder.

Observation: Pattern shifts, but signal passes through.

Remarks: Data taken in the late afternoon 21 February 1967; Temperatures in the teens. Extremely strong gusty wind. The cause of the shifting of patterns was discovered at the end of this test. A runaway fishing shed, blown across the cable by the wind, had pulled hydrophone HP-2 from the intended water depth of about 7 meters to the top where it was wedged in the hole drilled in the ice. In this position, the hydrophone is extremely sensitive to the shifting of the ice and variations of the water level in the hole.

Category 3:

Transmission: 80 Hz CW; Pulsed CW.

Transmitter: Two-transducer array.

Drive Power: Approximately 60 watts each.

Detection: By HP-1 and HP-2.

Reception:

a. Via PAR-JB-5 and PAR-HR-8. Lockin amplifiers switched to external reference, coherent detection position, for recording on the optical recorder.

b. Reception via PAR-JB-5 and PAR-HR-8. Lockin amplifier in internal reference non-coherent position for heterodyning received signals and recording with Sanborn Recorder, Model 322 (Fig. 7).

Observation: Signals came through strong and clear.

Remarks: Recordings made about midday 22 February 1967. Weather: Sunny and windy. Strong ice motion, a large crack developed in the ice between HP-1 and HP-2 letting water come onto the ice surface. (Shortly thereafter HP-2, the distant hydrophone 500 m offshore, was brought in)

Category 4:

Transmission: 82 Hz CW.

Transmitter: Single transducer XTD-H-2 alone.

Drive Power: 30 watts.

Soil Vibration: 5 in/s = 125 mm/sec (vertical soil vibration measured with MRM-1 Vibration Meter located 10 cm from XTD-H-2 piston edge.

Detection: By HP-1.

Received Signal: Hs = 10 mV ($\sim$ 1 microbar).

Ambient Noise: Hs = 2.7 mV ($\sim$ 0.27 microbar).

SKL Filter Setting: 60 Hz to 100 Hz; Keithly amplifier: (0 dB) ahead of Ballantine meter.

Remarks: Data taken 23 February 1967; Temperature: in the twenties (^{o}F); Snowing; Hydrophone HP-2 had been retrieved the day before due to the poor condition of the ice.

APPENDIX B

SIGNAL TRANSMISSION VIA ICE INTO WATER

DESCRIPTION OF SITES

1. Transmitter Site: On the ice about 165 to 200 meters offshore (Fig. 4). The four transducers in the linear array were set at 15 meters apart over a span of 45 meters (Transducer XTD-4 closest to shore, and transducer XTD-1 the farthest offshore).

2. Receiver Sites:

a. Hydrophone detector HP-1, the monitor hydrophone, 200 m offshore and halfway between transducer XTD-1 the transducer farthest offshore, and XTD-2 of linear 4-transducer array.

b. Hydrophone detector HP-2, the distant hydrophone, 500 m offshore, in line with the array.

These hydrophones were submerged 6 to 8 meters below the ice; hydrophone signal (Hs) measuring the recording equipment located in the van onshore; connection via cables.

EXPERIMENTS

Category 1:

Transmission Mode: 88 Hz CW.

Transmitter: Four-transducer array, XTD.

Radiation Pattern: Rotating via motor-driven phase shifter.

Drive Power: 0.9 watts each.

Detection Mode: By HP-1.

Received Signal: Levels and corresponding array phasing:

Hs_{max} = 72 mV (+16 dB) $\Delta\psi_{max} = 64°$

Hs_{min} = 4 mV (- 9 dB) $\Delta\psi_{min} = 40°$.

Ambient Noise: Hs = 2 mV (-15 dB).

SKL Filter Setting: 60 to 100 Hz; Keithly amplifier: 0 dB + Ballantine meter.

Recordings: HP-1 and HP-2 (See Fig. 8).

Evaluation: $\left(\frac{S+N}{N}\right)_{max}$ = 30 dB.

Remarks: Hs - dB levels refer to 1 microbar. Data taken 20 Feb 1967.

Category 2:

Transmission Mode: 250 Hz CW.

Transmitter: Four-transducer array.

Radiation Pattern: Rotating via motor-driven phase shifter.

Drive Power: Approximately 1 watt each.

Detection: By hydrophone HP-1.

Received Signal: Levels and corresponding array phasing:

Hs_{max} = 64 mV (+15 dB) $\Delta\varphi_{max} = 13^{\circ}$

Hs_{min} = 2.1 mV (-15 dB) $\Delta\varphi_{min} = 25^{\circ}$.

Ambient Noise: Hs = 1 mV (-20 dB).

SKL Filter Setting: 230 to 280 Hz; Keithly amplifier: 0 dB.

Recordings: HP-1 and HP-2 (See Fig. 9).

Evaluation: $\left(\frac{S+N}{N}\right)_{max}$ = 35 dB.

Remarks: Hs - dB levels refer to 1 microbar. Data taken toward noon, 20 February 1967; Temperatures ~10°F. Strong signals were also received by headphones using 20 dB gain on the Keithly amplifier.

Category 3:

Transmission Modes: 250 Hz Pulsed CW.

Transmitter: Four-transducer array.

Detection: By hydrophones HP-1 and HP-2, RC settings of PAR-JB-5 and HR-8, 0.1 sec and 0.3 sec respectively. Sample recordings of received pulse signals are shown in Fig. 10.

Ambient Noise: Levels were measured in mV as follows (22 February 1967):

Hydrophone #1	Hydrophone #2	Hydrophone #3
15 mV	1.3 (later 15) mV	wide band
3 mV	0.6 mV	60 - 120 Hz
2 mV	0.35 mV	230 - 280 Hz
6 mV	3 mV	900 - 1100 Hz .

Remarks: Pulse signals were received from hydrophones via SKL filters and Keithly amplifiers with PAR-JB-5 and HR-8 Lockin amplifiers using:

a. External reference (coherent detection).

b. Internal reference (non-coherent) heterodyne detection.

c. Internal reference (non-coherent) heterodyne detection with HR-8 locked to internal reference of PAR-JB-5. Relative phase stability between signals received from HP-1 and HP-2 is maintained.

d. CW signals heterodyned with internal reference on PAR-JB-5; both signals appear to have constant phase relationship. When

phasing of XTD array is rotated, hydrophone signals 1 and 2 change accordingly.

e. Keithly Amplifier: HP-1 set at 0 dB; HP-2 set at 20 dB.

Evaluation: The 88 Hz transmission received by distant HP-2, contained more ice-cracking noise than the 250 Hz transmission. It appears that the 80 Hz transmission from onshore via soil to water was less affected by ice-cracking noise than the 88 Hz transmission from the surface of the ice. Possible explanation: Noise vibrations emanating from the transmitter site are superimposed on the transmitted signal thereby adding to ambient noise from the receiver locale.

MEASUREMENTS OF TRANSDUCER INDUCED ICE VIBRATIONS VERSUS HYDROPHONE SIGNAL LEVELS (Hs)

Category 1, Measurements at 88 Hz CW:

XTD Drive Power: 0.9 watts each. Vertical ice vibrations measured with MBM-1 Vibration Meter at distances of 10 cm from the pistons of XTD-1 and XTD-2 respectively, and on the cradle for hydrophone HP-1 (Fig. 4).

SKL Filter Setting: 60 to 100 Hz; Keithly Amplifier: calibration +2 dB.

XTD-1 (alone): $\dot{\xi}_1 = 0.002$ in/s = 50 μ/sec. Hs = 48 mV.

XTD-2 (alone): $\dot{\xi}_2 = 0.0015$ in/s = 36 μ/sec. Hs = 36 mV.

XTD-1 and XTD-2 energized, (phased for max) yield: (Hs) max = 86 mV

and $\dot{\xi}_1 = 0.0026$ in/s = 60 μ/sec

$\dot{\xi}_2 = 0.0019$ in/s = 48 μ/sec

$\dot{\xi}_{cradle} = 0.0011$ in/s = 27 μ/sec.

Ambient Noise: Hs = 0.5 mV (-27 dB).

Remarks: Ambient noise vibration of ice below MBM-1 sensitivity.

Category 2, Measurements at 250 Hz CW:

XTD Drive Power: About 1 watt each.

Detection and Transmission Procedures: Set up the same as for 88 Hz measurements (see Category C-1) except SKL filter set at 230 to 280 Hz.

XTD-1 (alone): $\dot{\xi}_1 = 0.0054$ in/s = 0.133 mm/sec; Hs = 59 mV

XTD-2 (alone): $\dot{\xi}_2 = 0.016$ in/s = 0.4 mm/sec; Hs = 110 mV

XTD-1 and XTD-2 energized (phased for max) yield (Hs) max = 93 mV (see Remarks) $\dot{\xi}_{cradle} = 0.004$ in/s = 0.1 mm/sec.

Ambient Noise: Hs = 0.5 mV.

Remarks: XTD-2 exhibited strong audible coupling to air. (Cradle vibrations measurable only when both transducers are on.) These measurements were made on 21 February 1967; Temperature: $\sim 10^{o}$F. Weather: Windy, cloudy.

STACK TRANSDUCER AS TRANSMITTER (FIG. 3)

Category 1:

Transmission Mode: Voice.

Transmitter: Stack transducer* (Fig. 3).

Drive Power: ~ 50 watts (peak).

Detection: By hydrophone HP-1.

SKL Filter Setting: 250 to 1500 Hz; Keithly amplifier: (+40 dB) into earphones).

Observation: Voice communication excellent when used with above-mentioned filter.

Category 2:

Transmission: 1000 Hz CW, Pulsed CW; 4 periods on - 32 periods off.

Detection: By hydrophone HP-1.

SKL Filter Setting: 900 to 1100 Hz; 0 dB. Hs = 80 mV (Ballantine signal very strong), negligible noise; received pulse signal has perfect $\frac{\sin x}{x}$ envelope as seen on the scope.

Remarks: Data taken in the afternoon, 20 February 1967.

Category 3:

Transmission: 1000 Hz CW; Pulsed CW.

Transmitter: Stack transducer.

Drive Power: ~ 60 watts.

Detection: By hydrophones HP-1 and HP-2. Signals received by HP-2 are recorded on CEC Optical Recorder (Fig. 11).

Ambient Noise: Levels in 900 to 1100 Hz band.

a. Hydrophone HP-1 noise = 6 mV (~ 0.6 microbar).

b. Hydrophone HP-2 noise = 3 mV (~ 0.3 microbar).

Observation: Distant hydrophone signal (CW amplitude) was extremely strong (Fig. 11). This was the strongest signal obtained. Pulse mode came through clearly on distant hydrophone. (Monitor HP-1 channel out of order)

Remarks: Attempted voice communications to distant hydrophone HP-2 failed due to severe interference by ice noise (when the bandwidth was widened from 900 - 1100 Hz to 260 - 1500 Hz).

*This transducer was substituted for XTD-1 of the array and used alone. The stack transducer is an experimental wideband (artificially magnetostrictive) transducer made from stacked ceramic magnets, which are separated by plastic laminations having suitable compliance. Excitation is in this case provided by coils wrapped around the stack magnets, an inefficient improvisation. Actual refined model is presently under construction.

In accordance with test routines, stack transducer was lifted off the ice to check for possible electromagnetic coil-cable cross talk effects which are more likely to occur in this open-coil case. No such cross talk was observed. On the other hand, pressing the stack transducer onto the ice increased the volume of the hydrophone signal, which indicates improved coupling.

Data taken 22 February 1967; Weather: Sunny and windy. Strong ice motion, gaps began to develop about 300 to 500 m offshore.

MEASUREMENT OF STACK TRANSDUCER INDUCED ICE VIBRATIONS VERSUS HYDROPHONE SIGNAL LEVELS

Transmission: 1000 Hz CW.

Stack Drive Power: 66 V, 1.3 amp. (at input of 1000 feet feed cable).

Measurements: Vertical ice vibration at 30 cm from stack transducer. MEM-1 Vibration Meter reading: $\not{v}$ = 0.0035 in/s = 87 μ"/sec. Corresponding hydrophone HP-1 signal Hs = 56 mV ($\sim$ 5 microbars).

Ambient Noise: Hs = 1 mV ($\sim$ 0.1 microbar), (Bandwidth 900 to 1100 Hz).

Remarks: Data taken 21 February 1967; Temperature: In the teens (^{o}F), Weather: Cloudy, strong winds.

APPENDIX C

CW - SCATTER EXPERIMENTS

EXPERIMENTAL SETUP

Shown by diagram in Fig. 12.

Transmission Mode: 250 Hz CW from either:

a). All four transducers (1 w each) phased to originally yield a minimum of the signal received by the hydrophone. Here the scatter object is submerged beneath the center of the square array (Side scatter experiment), or

b). Only one transducer (XTD-1) energized. Here the scatter object is submerged between XTD-1 and the hydrophone location (Forward scatter experiment).

Procedure: The scatter object, in our case a rubber mat approximately 1.5 cm thick, 2 m long, and 1 m wide, weighted with old batteries, is lowered by rope into the water as shown in Fig. 12. As the rubber mat sinks to the bottom or is pulled up to the surface, phase variations on the 250 Hz signal are recorded (via the HR-8 Lockin amplifier) on the Sanborn 322 Recorder.

SIDE SCATTER EXPERIMENT

Results of the side scatter experiment are shown by the recording in Fig. 13. The peak phase deviation as calibrated is 25° and occurs when the rubber mat (scatterer) is halfway down (15 meters) between the ice and the bottom.

FORWARD SCATTER EXPERIMENT

Results of the forward scatter experiment are shown by the recording in Fig. 14. Here the phase deviation versus depth of scatterer is double-peaked. The peak phase deviations are of the same order of magnitude, i.e., 20° to 30°.

Remarks: With regard to the double-humped and single-humped phase deviation curves for the forward and side scatter experiments respectively, note that the density and/or absorption-type scatter volume has a null of its secondary radiation pattern along the direction of the incident wave and a peak in a direction perpendicular to the incident wave (See Appx. E).

The influence of possible standing waves between the ice and lake bottom is unknown at present. An attempt to solve this problem by use of a submarine model for recording scatter from a horizontally moving scatter object failed. Batteries of the submarine failed at the low temperatures. In the next attempt, external dc-power will be used to feed the submarine motor via wires from a battery-charger.

EFFECTS OF AIR BUBBLES BETWEEN THE ICE AND WATER*

CO_2, blown via a long hose from a fire extinguisher below the ice, was used to determine possible scatter effects (250 Hz); and possible deterioration

*Efforts to contain the CO_2 in a weather balloon submerged below the ice failed, as these balloons burst.

of 250 Hz signal transmissions. Initial release of air bubbles appears more like a noiseburst disturbance than like scatter (Fig. 15). No appreciable change in signal strength occurred, even though a large sheet of CO_2 gas was formed between the ice and water at the transmitter site (For slight phase change see Fig. 15).

Remarks: Data taken on 22 February 1967 towards nightfall. Attempts to run a 1000 Hz scatter experiment using the stack transducer the next morning had to be abandoned because of equipment difficulties under worsening weather conditions.

APPENDIX D

80 Hz SCATTER EXPERIMENT FROM ONSHORE

EXPERIMENTAL SETUP

80 Hz Transmission Via Soil Into Water From Large Transducer (Fig. 2):

Procedures using a receiver recorder system and a rubber mat as a scatter obstacle were similar to those previously described in Appx. C. Results were negative.

Remarks: This was only a very brief experiment made while packing up on 23 February 1967. The relative locations of the scatter object and hydrophone receiver do not appear to be correct for this case. Probing of seismic waves emanating from the shore and bottom of the lake into the water is required for intelligent exploration of seismic-sonic transmission for detection of scatter objects in water.

APPENDIX E

THEORETICAL VERIFICATION OF RESULTS OF THE SCATTER EXPERIMENTS

Acoustic scatter radiation due to the presence of an obstacle is described by the following formula (for its derivation, see Appendix F):

$$p_s = \frac{p_o}{4\pi k_o R} \cdot e^{-j(\omega t - k_o R)} \cdot$$

$$\cdot \frac{\sin k_o \frac{\ell}{2}\left(1-\frac{x}{R}\right)}{k_o \frac{\ell}{2}\left(1-\frac{x}{R}\right)} \cdot \frac{\sin k_o \frac{b}{2}\frac{y}{R}}{k_o \frac{b}{2}\frac{y}{R}} \cdot \frac{\sin k_o \frac{h}{2}\cdot\frac{z}{R}}{k_o \frac{h}{2}\frac{z}{R}} \cdot \qquad [1]$$

$$\cdot \left\{ k_o^3 \ell b h \left[2\frac{\Delta c}{c_o} + \frac{\Delta \rho}{\rho_o}\left(1-\frac{x}{R}\right)\right] \right.$$

$$\left. + a \cdot \frac{e^{j\frac{\pi}{2}}}{2} \cdot k_o^2 \left[\ell b + \ell h + b h\right]\left(1-\frac{x}{R}\right) \right\}$$

where the symbols (also used in Appx. F) denote:

p_s.....pressure amplitude of the scattered wave

P_o.....pressure amplitude of incident planar wave propagating along the x direction

$k_o = \frac{2\pi}{\lambda o}$....propagation constant; $\omega = k_o c_o$

ℓ, b, h.....dimensions of the obstacle

R.....distance between point of observation (xyz) of p_s and the scatter obstacle

c_o.....sound velocity, ρ_o density of the water

Δc and $\Delta \rho$ ..deviations from c_o and ρ_o respectively within the volume ℓ, b, h of the scatter obstacle

a.....sound absorption coefficient of the scatter obstacle (For its definition, see Appx. F, Eq. (29).

During experiments, incident acoustic waves were not perfectly planar; however, for the distances used in the experiments, wave fronts can be considered sufficiently planar to warrant use of Formula (1).

It is also safe to assume that the obstacle, the water-soaked foam-rubber mat, acts essentially as an absorber. In other words, the foam-rubber mat

does not present an appreciable inhomogeneity of velocity and density, i.e., $\Delta c \doteq c$. $\Delta \rho \doteq \rho$ in Formula (1). Consequently, only the third term of Formula (1), involving the absorption coefficient a, is used for subsequent calculation of scatter-induced phase variations of the 250 Hz CW transmission. (Notice that for R = x, i.e., in the direction of the incident wave, p_s vanishes when the obstacle is an absorber. This agrees with results of the forward scatter experiment.)

In the following discussion of the side scatter problem, we must consider the magnitudes and phases of the direct wave and scattered wave at the location of the hydrophone. The essential facts of the side scatter experiment were: The direct wave was minimized while the primary wave (along the x direction) towards scatter obstacle was maximized by controlling the drive voltages of the seismic transducers on the ice. In other words, the hydrophone was located in a minimum and the scatter object in a maximum of the acoustic radiation pattern. Thus, the hydrophone received a pressure

$$p_{HS} = m \frac{p_0 e^{j k_c \sqrt{x^2+y^2}}}{4\pi k_c \sqrt{x^2+y^2}} + \left(\frac{p_0 e^{j k_0 x}}{4\pi k_0 x}\right) \cdot \frac{e^{j k_0 y}}{4\pi k_0 y} \cdot \frac{\sin k_0 \frac{l}{2}}{k_0 \frac{l}{2}} \cdot \frac{\sin k_0 \frac{b}{2}}{k_0 \frac{b}{2}} \cdot e^{-j\frac{\pi}{2}} a \frac{k_0^2}{2} [lb + lh + bh] \qquad [2]$$

The first term in Eq. (2) represents the direct pressure wave ($p_{dir.}$). The factor m denotes the ratio of minimum to maximum of the direct acoustic radiation pattern of the square array of seismic transducers. The second term represents the scattered wave that emanates from the scatter object.

$\frac{p_0 e^{j k_0 x}}{4\pi k_0 x}$ is the pressure incident on the scatter object. From Eq. (2) the relative scatter induced change of the hydrophone signal follows as:

$$\frac{p_{HS}}{p_{dir}} = \left[1 - A \sin k_c \left(x + y - \sqrt{x^2+y^2}\right)\right] + j\left[A \cos k_c \left(x + y - \sqrt{x^2+y^2}\right)\right] \qquad [3]$$

where

$$A = a\,\frac{k_o^2}{2}\left[b\ell + \ell h + h b\right] \cdot \frac{\sqrt{x^2+y^2}}{mx} \cdot \frac{1}{4\pi k_o y} \cdot \frac{\sin k_o \frac{\ell}{2}}{k_o \ell/2} \cdot \frac{\sin k_o \frac{b}{2}}{k_o b/2} \cdot \frac{\sin k_o \frac{h}{2}}{k_o h/2} \quad . \qquad [4]$$

The scatter induced phase change $\Delta\varphi_s$ is then given by

$$\tan \Delta\varphi_s = \frac{A \cos k_o \left(x+y-\sqrt{x^2+y^2}\right)}{1 - A \sin k_o \left(x+y-\sqrt{x^2+y^2}\right)} \quad . \qquad [5]$$

Substitution of the following experimental quantities:

Dimensions of the foam-rubber mat.....	ℓ = 2 m, h = 1 m, b = 0.015 m
An assumed absorption coefficient.....	a = 1
The wave propagation constant.....	k_o = 1 m^{-1}
Depth of submersion of the foam-rubber mat below the square array of transducers....	x = 6 m
Distance from mat to hydrophone.....	y = 30 m
The min-max ratio of the radiation pattern.	m = 1/20 (-26 dB)

yields

$$\tan \Delta\varphi_s \doteq 0.2 \quad .$$

This results in a phase change $\Delta\varphi_s$ of approximately 12 degrees.

Considering the crudeness of the theoretical model used for derivation of the scatter (Formula (1), Appx. F), agreement within the order of magnitude of the experimental value (25 degrees) is satisfactory.

In this respect, it is necessary to emphasize the meaning of the absorption coefficient "a". For derivation of Formula (1), Appx. F, we have used the relaxation time associated with absorption of diffuse sound by the walls of a solid body as equal to the relaxation time associated with viscous absorption of monochromatic sound. Consequently, experimental values for the scattered pressure p_s should be larger than calculated values by at least a factor 2; since monochromatic power flow density is four times the diffuse power flow density for the same energy density (See Appx. F, Formulas (27) and (28)).

APPENDIX F

DERIVATION OF ACOUSTIC SCATTER FORMULA

Derivation of the scatter formula proceeds from the following equations:

Eulers Equation: $$\rho \frac{d\bar{v}}{dt} + K\bar{v} = -\text{grad}\, p \qquad [1]$$

Continuity Equation: $$\frac{\partial \rho}{\partial t} + \text{div}\, \rho \bar{v} = 0 \qquad [2]$$

Equation of State: $$p = f(\rho) = a\rho^{\kappa} \qquad [3] \; .$$

By considering incremental changes of pressure p and velocity v, as well as local variations (inhomogeneities) of the sound propagation velocity c, the density ρ and the viscosity K in the acoustic medium, one arrives at an inhomogeneous wave equation for the acoustic pressure.

The driving function of this wave equation contains the inhomogeneities of c, ρ and K .

Solutions of this inhomogeneous wave equation are obtained by successive approximations, involving in our case perturbation of an original plane wave solution.

We proceed as indicated:

$$p = p_0 + \frac{dp}{dt}\,dt = p_0 + p_1$$

$$f(\rho) - f(\rho_0) = f'(\rho_0) + \left[\frac{df}{d\rho}\right]_{\rho=\rho_0} \cdot \rho_1 =$$

$$= f(\rho_0) + \frac{\gamma}{\rho_0}\left(f(\rho_0)\right)\rho_1 =$$

$$= \rho_0 + \frac{\gamma \rho_0}{\rho_0}\cdot \rho_1$$

$$p_1 = \frac{\gamma \rho_0}{\rho_0}\rho_1 = \kappa^2 \rho_1 \qquad [4]$$

$$\frac{d}{dt} = \frac{\partial}{\partial t} + \bar{v}\cdot\nabla$$

$$\frac{d\rho_1}{dt} = \frac{\partial \rho_1}{\partial t} + \underbrace{(\bar{v}_1\cdot\nabla)\rho_1}_{\text{small of second order neglected}}$$

$$\frac{d\rho}{dt} = \frac{\partial \rho}{\partial t} + \bar{v}_1\cdot\nabla\rho = \frac{\partial \rho_1}{\partial t} + \bar{v}_1\cdot\nabla\rho \qquad \text{small of first order is retained}$$

from [1] [2]

$$\rho\frac{\partial \bar{v}_1}{\partial t} + \kappa \bar{v}_1 = -\,\mathrm{grad}\, p_1$$

$$\frac{\partial \rho_1}{\partial t} + \mathrm{div}(\rho \bar{v}_1) = 0 \qquad [5]$$

$$\frac{\partial}{\partial t}\mathrm{div}(\rho \bar{v}_1) = \mathrm{div}\left(\rho \frac{\partial \bar{v}_1}{\partial t}\right) + \mathrm{div}\left(\frac{\partial \rho}{\partial t}\bar{v}_1\right)$$

$\mathrm{div}\left(\frac{\partial \rho}{\partial t}\bar{v}_1\right)$ → small, of second order, neglected.

$$= -\frac{\partial^2 \rho_1}{\partial t^2}$$

$$= \mathrm{div}(-\mathrm{grad}\, p_1 - \kappa \bar{v}_1) \qquad [6]$$

[4][5] $$\frac{dp}{dt} = \kappa^2 \frac{d\rho}{dt} = \kappa^2\left[\frac{\partial \rho_1}{\partial t} + \bar{v}_1\cdot\nabla\rho\right] =$$

$$= \frac{\partial p_1}{\partial t}$$

$$\frac{\partial^2 p_1}{\partial t^2} = \frac{1}{\kappa^2}\frac{\partial^2 p_1}{\partial t^2} - \frac{\partial}{\partial t}(\bar{v}_1\cdot\nabla\rho) \qquad [7]$$

[6][7] $$\frac{1}{\kappa^2}\frac{\partial^2 p_1}{\partial t^2} - \frac{\partial}{\partial t}(\bar{v}_1\cdot\nabla\rho) = \mathrm{div}(\mathrm{grad}\, p_1 + \kappa \bar{v}_1)$$

$$\frac{1}{\kappa^2}\frac{\partial^2 p_1}{\partial t^2} - \frac{\partial \bar{v}_1}{\partial t}\cdot\nabla\rho = \mathrm{div}\,\mathrm{grad}\, p_1 + \mathrm{div}\,\kappa\bar{v}_1 \qquad [8]$$

(note $(\bar{v}_1\cdot\nabla\frac{\partial \rho}{\partial t})$ small of second order, neglected)

from [5] $$\frac{\partial \bar{v}_1}{\partial t} + \frac{\kappa}{\rho}\bar{v}_1 = -\frac{1}{\rho}\mathrm{grad}\, p \qquad [8']$$

(note: $\frac{\kappa}{\rho} = \frac{1}{\tau}$; τ relaxation time)

consider time dependence $\sim e^{-j\omega t}$

$$-j\omega \bar{v}_1 + \frac{\kappa}{\rho}\bar{v}_1 = -\frac{1}{\rho}\,\mathrm{grad}\,p_1$$

$$\bar{v}_1 = \frac{-\mathrm{grad}\,p_1}{\kappa - j\omega\rho} \qquad [9]$$

$$\frac{\partial \bar{v}_1}{\partial t} = +\frac{j\omega\,\mathrm{grad}\,p_1}{\kappa - j\omega\rho} \qquad [9']$$

$$(\nabla\cdot\bar{v}_1) = \frac{-\mathrm{div}\,\mathrm{grad}\,p_1}{\kappa - j\omega\rho} + \left(\mathrm{grad}\,p_1 \cdot \frac{\mathrm{grad}(-j\omega\rho+\kappa)}{(-j\omega\rho+\kappa)^2}\right)$$

$$\mathrm{div}\,\kappa\bar{v}_1 = (\mathrm{grad}\,\kappa\cdot\bar{v}_1) + \kappa\,\mathrm{div}\,\bar{v}_1$$

$$\mathrm{div}\,\kappa\bar{v}_1 = \frac{-\mathrm{grad}\,\kappa\cdot\mathrm{grad}\,p_1}{\kappa - j\omega\rho} + \qquad [9'']$$

$$+\kappa\,\frac{\mathrm{grad}\,p_1\cdot\mathrm{grad}(\kappa - j\omega\rho)}{}$$

$$-\frac{\kappa}{\kappa - j\omega\rho}\,\mathrm{div}\,\mathrm{grad}\,p_1$$

---

set $\quad \kappa = \kappa_0 + \Delta\kappa$

then $\quad \frac{1}{\kappa} \doteq \frac{1}{\kappa_0}\left(1 - \frac{\Delta\kappa}{\kappa_0}\right) \qquad [10]$

$$\frac{1}{\kappa^2} \doteq \frac{1}{\kappa_0}\left(1 - 2\,\frac{\Delta\kappa}{\kappa_0}\right)$$

$\Delta\kappa$ .. inhomogeneity associated with the scatter volume.

[8][9][10]

$$\left[\frac{\omega^2}{\kappa_0^2} + \left(1 - \frac{\kappa}{\kappa - j\omega\rho}\right)\nabla^2\right]p_1 = \qquad [11]$$

$$= 2\,\frac{\omega^2}{\kappa_0^2}\cdot\frac{\Delta\kappa}{\kappa_0}\cdot p_1 +$$

$$\nabla p_1 \cdot\left[\frac{\nabla(\kappa - j\omega\rho)}{\kappa - j\omega\rho} - \kappa\cdot\frac{\nabla(\kappa - j\omega\rho)}{(\kappa - j\omega\rho)^2}\right]$$

similarly to [10] set $\quad \rho = \rho_0 + \Delta\rho$

$$\kappa = \kappa_0 + \Delta\kappa \qquad [11']$$

[11] [11']

$$\left[\frac{\omega^2}{\kappa_0^2} + \left(1 - \frac{K_0 + \Delta K}{K - j\omega\rho}\right)\nabla^2\right] p_1 =$$

[12]

$$= 2\frac{\omega^2}{\kappa_0^2}\frac{\Delta c}{c_0} p_1 +$$

$$+ \nabla p_1 \cdot \left[\frac{\nabla(\Delta K - j\omega\Delta\rho)}{K - j\omega\rho} + (K_0 + \Delta K)\frac{\nabla(\Delta K - j\omega\Delta\rho)}{(K - j\omega\rho)^2}\right]$$

note: in a first-order approximation $\Delta\rho$ and ΔK may be neglected relative to ρ_0 and K_0. But $\nabla(\Delta\rho)$ and $\nabla(\Delta K)$ must be retained; note that

$$\left|\frac{\Delta K}{j\omega\rho_0}\right| \ll 1 \qquad [12']$$

and $\frac{\omega}{\kappa_0} = k_0$.

Hence the first-order approximation of [12] using $K_0 = 0$ (water) reads as follows:

---

[12] [12']

[13]

$$(k_0^2 - \nabla^2) p_1 = 2k_0^2 \frac{\Delta c}{c_0} p_1 + \frac{1}{\rho_0}\nabla p_1 \cdot \nabla(\Delta\rho) - \frac{1}{j\omega\rho_0}\nabla p_1 \cdot \nabla(\Delta K)$$

set $= 4\pi Q_{sp}$ [14]

consider $p_1 = p_p + p_s$

p_p .. primary

p_s .. secondary (scattered) wave $\ll p_p$

split [13] into

$$(k_0^2 + \nabla^2) p_p = 0 \qquad [15]$$

and

$$(k_0^2 + \nabla^2) p_s = 4\pi Q_{sp} + \text{neglected terms of higher orders of smallness involving } p_s \text{ and } \nabla p_s \qquad [16]$$

then

$$p_s = \int_{Vol} \frac{Q_{sp}\left(t - \frac{r}{c_0}\right)}{r} dVol \qquad [17]$$

where $(\xi\eta\zeta)$ are the coordinates of Q_{sp} and
(xyz) the coordinates of p_s as shown below:

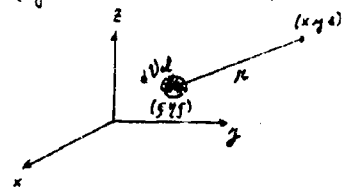

Use as a solution of [15]

$$p_p = P_0 e^{-j(\omega t - k_0 x)} \qquad [18]$$

a plane wave propagating in the x direction.
Get:

$$\nabla p_p = j \bar{e}_x P_0 k_0 e^{-j(\omega t - k_0 x)} \qquad [19]$$

($\bar{e}_x$ unit vector along x) [20]

then.

$$\nabla p_p \cdot \nabla(\Delta p) = j k_0 P_0 \left[\frac{\partial}{\partial x}(\Delta p)\right] e^{-j(\omega t - k_0 x)}$$

$$\nabla p_p \cdot \nabla(\Delta K) = j k_0 P_0 \left[\frac{\partial}{\partial x}(\Delta K)\right] e^{-j(\omega t - k_0 x)}$$

at $(\xi\eta\zeta)$ from [13][14][19][20]

$$Q_{sp} = \frac{P_0}{4\pi} e^{-j(\omega t - k_0 \xi)} \qquad [21]$$

$$\cdot \left[2 k_0^2 \frac{\Delta c}{c_0} + \frac{j k_0}{p_0}\left(\frac{\partial}{\partial \xi}(\Delta p)\right) - \frac{j k_0}{j\omega p_0}\left(\frac{\partial}{\partial \xi}(\Delta K)\right)\right]$$

introduction of the retardation $t \to (t - \frac{R}{c_0})$
and [21] into [17] gives

$$p_s = \frac{P_0 e^{-j\omega t}}{4\pi} \cdot \qquad [22]$$

$$\cdot \iiint_{Vol} \frac{\left[2k_0^2 \frac{\Delta c}{c_0} + \frac{j k_0}{p_0}\frac{\partial \Delta p}{\partial \xi} - \frac{j k_0}{j\omega p_0}\frac{\partial \Delta K}{\partial \xi}\right]}{R} \cdot e^{+j k_0 (R + \xi)} \cdot d\xi\, d\eta\, d\zeta$$

shift of the coordinate system as indicated below. (l h b dimensions of the scatter volume)

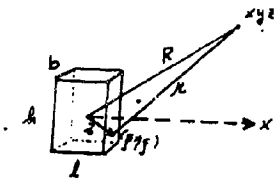

and using $\bar{R} = \bar{s} + \bar{r}$ $\bar{r} = \bar{R} - \bar{s}$

$$r^2 = R^2 + s^2 - 2\bar{R}\cdot\bar{s} \doteq \text{approximate}$$

$$\doteq R^2 - 2\bar{R}\cdot\bar{s} \quad \text{for } |\bar{s}| \ll R$$

$$r \doteq R\sqrt{1 - 2\frac{\bar{R}\cdot\bar{s}}{R^2}} \doteq R - \frac{\bar{R}\cdot\bar{s}}{R}.$$

where $\bar{R}\cdot\bar{s} = x\xi + y\eta + z\zeta$

then in [22]

$$r + \xi = R + \xi\left(1 - \frac{x}{R}\right) - \eta\frac{y}{R} - \zeta\frac{z}{R}$$

$$p_s \doteq \frac{P_0}{4\pi R} \cdot e^{-j(\omega t - k_0 R)} \qquad [23]$$

$$\cdot \iiint \left[2k_0^2 \frac{\Delta\varepsilon}{\varepsilon_0} - \frac{1}{\rho_0 c_0}\left(\frac{\partial}{\partial t}(\Delta\kappa - j\omega\Delta\rho)\right)\right] \cdot$$

Vol (16R)

$$\cdot e^{+jk_0\left[\xi\left(1 - \frac{x}{R}\right) - \eta\frac{y}{R} - \zeta\frac{z}{R}\right]} \cdot d\xi\, d\eta\, d\zeta$$

For an explicit solution of [23] consider $\Delta\varepsilon$ $\Delta\rho$ $\Delta\kappa$ be constant with in the scatter volume

$$-\tfrac{l}{2} \le \xi \le +\tfrac{l}{2}$$

$$-\tfrac{b}{2} \le \eta \le +\tfrac{b}{2}$$

$$-\tfrac{h}{2} \le \zeta \le +\tfrac{h}{2} \qquad [24]$$

then $\Delta\varepsilon$ $\Delta\rho$ $\Delta\kappa$ are defined by jumpfunctions

e.g. $\Delta\rho = \rho_1\left[\varepsilon\left(\xi + \tfrac{l}{2}\right) - \varepsilon\left(\xi - \tfrac{l}{2}\right)\right]$ as indicated by

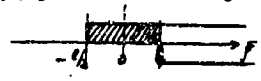

[25]

then $\frac{\partial}{\partial \xi} \Delta p = \rho_1 [\delta(\xi + \ell/2) - \delta(\xi - \ell/2)]$

where δ .. Dirac's function

this gives the scattered pressure :

[26]

$$p_s = \frac{F_0}{4\pi R} \cdot e^{-j(\omega t - k_0 R)} \cdot (l b h) \cdot k_0^2 \cdot$$

$$\cdot \frac{\sin k_0 \frac{l}{2}\left(1 - \frac{x}{R}\right)}{k_0 \frac{l}{2}\left(1 - \frac{x}{R}\right)} \cdot \frac{\sin k_0 \frac{b}{2} \frac{y}{R}}{k_0 \frac{b}{2} \frac{y}{R}} \cdot \frac{\sin k_0 \frac{h}{2} \frac{z}{R}}{k_0 \frac{h}{2} \frac{z}{R}} \cdot$$

$$\cdot \left[2 \frac{\Delta \rho}{\rho_0} + \left(\frac{\Delta \rho}{\rho_0} - \frac{\Delta \kappa}{j \omega \rho_0}\right)\left(1 - \frac{x}{R}\right)\right]$$

as a matter of physical interpretation the absorption coefficient α is introduced by expressing $\frac{\rho_0}{\Delta \kappa}$ as an equivalent relaxation time of a solid body.

For this purpose we use Kirchhoff's law

$$(\text{watt}/m^2)\ \mathcal{P} = \mathcal{E}\, \kappa\ (\text{watt sec}/m^3 \cdot m/\text{sec}). \quad [27]$$

Power flow through a solid angle Ω

$$d\mathcal{P} = d\mathcal{E}\, \kappa \cos\theta$$

and $d\mathcal{E} = \mathcal{E} \cdot \frac{d\Omega}{4\pi} = \mathcal{E} \cdot \frac{\sin\theta\, d\theta}{2}$

then $d\mathcal{P} = -\frac{\mathcal{E}\kappa}{4} d(\cos^2\theta)$

and the total diffuse power flow density

$$\mathcal{P} = -\frac{\mathcal{E}\kappa}{4}\left[\cos^2\theta\right]_{\theta=0}^{\theta=\frac{\pi}{2}} = +\frac{\mathcal{E}\kappa}{4}. \quad [28]$$

The absorption coeffient "α" denotes the fraction of the total incident power that is absorbed by the surface of the body.

$$P_a = a \cdot S \frac{\mathcal{E} c}{4} . \qquad [29]$$

The relaxation time for the energy decay in a volume V follows from

$$\frac{d}{dt} \mathcal{E} V + a S \frac{\mathcal{E} c}{4} = 0$$

$$\mathcal{E} = \mathcal{E}_0 e^{-a \frac{Sc}{4V} t} \qquad [30]$$

which gives

$$T = \frac{4V}{aSc} . \qquad [31]$$

on the other hand viscous damping gives $T = \frac{\rho_0}{\Delta K}$ [31']

hence we replace in [26] [32]

$\frac{\Delta K}{\rho_0}$ by $\frac{aSc}{4V} = a \frac{c}{2} \left(\frac{1}{l} + \frac{1}{b} + \frac{1}{h} \right)$

this gives the final result (the scalar formula[1] of Appendix E)

$$\varphi_S = \frac{P_0}{4\pi k_0 R} \cdot e^{-j(\omega t - k_0 R)} \qquad [33]$$

$$\cdot \frac{\sin k_0 \frac{l}{2}\left(1 - \frac{x}{R}\right)}{k_0 \frac{l}{2}\left(1 - \frac{x}{R}\right)} \cdot \frac{\sin k_0 \frac{b}{2} \frac{y}{R}}{k_0 \frac{b}{2} \frac{y}{R}} \cdot \frac{\sin k_0 \frac{h}{2} \frac{z}{R}}{k_0 \frac{h}{2} \frac{z}{R}} \cdot$$

$$\cdot \left\{ k_0^3 lbh \left[2 \frac{\Delta c}{c_0} + \frac{\Delta \rho}{\rho_0} \left(1 - \frac{x}{R}\right) \right] + \right.$$

$$\left. + e^{j\frac{\pi}{2}} \cdot a \cdot \frac{k_0^2}{2} [lb + lh + bh] \left(1 - \frac{x}{R}\right) \right\} .$$

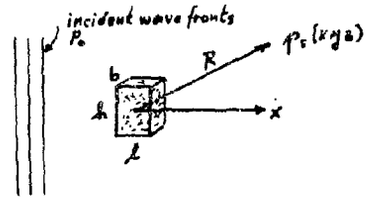

UNCLASSIFIED
Security Classification

DOCUMENT CONTROL DATA - R & D

(Security classification of title, body of abstract and indexing annotation must be entered when the overall report is classified)

1. ORIGINATING ACTIVITY (Corporate author)
U. S. Army Electronics Command
Fort Monmouth, New Jersey

2a. REPORT SECURITY CLASSIFICATION
UNCLASSIFIED

2b. GROUP

3. REPORT TITLE
COMMUNICATION AND TARGET DETECTION THROUGH ICE BY MEANS OF SEISMIC ACOUSTIC SIGNALS

4. DESCRIPTIVE NOTES (Type of report and inclusive dates)
Technical Report

5. AUTHOR(S) (First name, middle initial, last name)
Kurt Ikrath, Ronald F. Johnson, William Kennebeck, Kenneth J. Murphy, Robert Ridgeway, and Leonard Stascavage

6. REPORT DATE	7a. TOTAL NO. OF PAGES	7b. NO. OF REFS
October 1967	45	6

8a. CONTRACT OR GRANT NO.	9a. ORIGINATOR'S REPORT NUMBER(S)
b. PROJECT NO. 1P0 14501 B31A 01 43	ECOM-2900
c.	9b. OTHER REPORT NO(S) (Any other numbers that may be assigned this report)
d.	

10. DISTRIBUTION STATEMENT (2)

This document is subject to special export controls and each transmittal to foreign governments or foreign nationals may be made only with prior approval of: CG, U.S. Army Electronics Command, Fort Monmouth, N. J. Attn: AMSEL-XL-C

11.	12. SPONSORING MILITARY ACTIVITY (AMSEL-XL-C)
	Institute for Exploratory Research Fort Monmouth, New Jersey 07703

13. ABSTRACT

Seismic-acoustic signal transmission experiments, employing novel seismic transducers on land and lake ice as transmitters and conventional hydrophones in water beneath the ice as receivers, are described. The observed influences of wave excitation and propagation phenomena on the signal character of transmissions through earth, ice, and water are discussed. Applications of seismic-acoustic systems for communications and target detection are indicated.

DD FORM 1 NOV 68 1473 REPLACES DD FORM 1473, 1 JAN 64, WHICH IS OBSOLETE FOR ARMY USE.

(3)

UNCLASSIFIED
Security Classification

UNCLASSIFIED
Security Classification

14. KEY WORDS	LINK A		LINK B		LINK C	
	ROLE	WT	ROLE	WT	ROLE	WT
Geophysics						
Seismic						
Acoustic						
Lake Ice						
Wave Propagation						
Target Detection						
Transducers						
Hydrophones						

ESC-FM 5145-67

UNCLASSIFIED
Security Classification